# Origin of the Anomalous Magnetic Behavior in Single Crystal $Fe_3O_4$ Films

D. T. Margulies,[1,*] F. T. Parker,[1] M. L. Rudee,[1] F. E. Spada,[1] J. N. Chapman,[2] P. R. Aitchison,[2] and A. E. Berkowitz[1]
[1]*Center for Magnetic Recording Research, University of California at San Diego, La Jolla, California 92093-0401*
[2]*Department of Physics and Astronomy, University of Glasgow, Glasgow, G12 8QQ, United Kingdom*
(Received 10 June 1997)

Antiphase boundaries (APBs) were observed in $Fe_3O_4$ single crystal films grown on MgO. The APBs are an intrinsic consequence of the nucleation and growth mechanism in films. Across an APB, the intrasublattice superexchange coupling is greatly strengthened, while the intersublattice superexchange coupling is weakened, reversing the dominant interaction from that found in the bulk. Thus the APB separates oppositely magnetized regions, consistent with Lorentz microscopy measurements. The APBs induce very large saturation fields and nearly random magnetization distribution in zero field. [S0031-9007(97)04642-5]

PACS numbers: 75.70.Ak

The scientific and technological importance of spinel structure ferrites has led many investigators [1–9] to examine single crystal spinel films. Much emphasis has been placed on the growth of $Fe_3O_4$ single crystalline films by various deposition methods using MgO as a substrate. We recently showed [1] that the magnetic properties of single crystal $Fe_3O_4$ films grown by sputter deposition, molecular-beam epitaxy, and evaporation deviate from bulk single crystal behavior; in particular, they exhibit very large saturation fields and quasirandom zero-field magnetic moment distributions. This Letter describes how the modified superexchange interactions at the antiphase boundaries (APBs) observed in the $Fe_3O_4$ films produce the puzzling magnetic behavior. The APBs, or stacking defects in the cation sublattices, are an intrinsic consequence of the nucleation and growth mechanism of films, which suggests that these boundaries, and thus the anomalous magnetic behavior, should be present for all spinel films grown on MgO independent of deposition technique.

Both $Fe_3O_4$ and MgO crystallize with the O atoms in an approximately face-centered cubic (fcc) lattice. In $Fe_3O_4$, the Fe atoms occupy specific tetrahedral (*A*) and octahedral (*B*) sites. The similar *d* spacings of the O lattices in MgO and $Fe_3O_4$ (mismatch $\sim 0.3\%$) make MgO an excellent template for the growth of epitaxial single crystal $Fe_3O_4$ films. However, it is important to note that the $Fe_3O_4$ unit cell (lattice parameter $a_0 = 8.3967$ Å) is nearly twice the size of the MgO unit cell ($a_0 = 4.213$ Å) due to the more complicated cation arrangement in the former. Structural characterization of $Fe_3O_4$ films grown on MgO shows that they are indeed monocrystalline, and that they grow with the same orientation as the substrate [1]. Rocking curve measurements on sputtered films show that the film reflections are exceptionally sharp, with a $\sim 0.01°$ full-width at half-maximum, demonstrating uniform *d* spacing in the films and indicating apparently defect-free crystals.

However, the magnetic properties of the films grown by sputter deposition, molecular-beam epitaxy, and evaporation differ markedly from those expected for single crystal $Fe_3O_4$ with bulk behavior [1]. The magnetization of the films is not saturated in fields of 70 kOe, although the bulk $Fe_3O_4$ anisotropy field is $\sim 310$ Oe. The high field differential susceptibility appears to be isotropic. Conversion electron Mössbauer spectroscopy spectra of the films obtained in zero field show considerable out-of-plane magnetization, although the moments would be expected to lie in the film plane due to the large shape anisotropy. Torque curves taken with the field rotating both in and out of the film plane are unsaturated at 20 kOe. However, the symmetries and extrapolated values of the anisotropies measured by the torque curves are consistent with those of single crystal bulk $Fe_3O_4$ subjected to in-plane tensile strain of the magnitude measured in the films [1], arising from the pseudomorphic growth of $Fe_3O_4$ on MgO. This shows that shape anisotropy (anisotropy field $\sim 6$ kOe) is the dominant global anisotropy and that the magnitudes of all anisotropies are much less than that needed to produce the anomalous magnetic behavior.

We have shown [1] that the isotropic high field differential susceptibility, due to the very large saturation field, is relatively independent of temperature from 10–300 K. This result indicates that the origin for the anomalous behavior is related to the exchange interactions in the films. Although the presence of strain-induced changes in the exchange interactions could produce a noncollinear spin structure, we have determined that the hyperfine fields at the *A* and *B* sites are the same in the films at 296 K as they are in bulk specimens [1]. Furthermore, transmission Mössbauer measurements of the temperature dependence of the hyperfine fields in a 6.6 $\mu$m film grown on $\langle 100 \rangle$ MgO show that the ratios of the hyperfine fields at 296 to 130 K for the *A* and *B* sites are 0.966(3) and 0.953(3), respectively, while in bulk specimens the respective ratios [10] are 0.970(3) and 0.952(3). The uncertainties in the last digit are given in parentheses next to the values. Since the temperature dependence of the hyperfine fields is determined by the exchange integrals [10] and angles between spins, it appears as if there is no

 0031-9007/97/79(25)/5162(4)$10.00 

difference on average between these parameters in films and bulk specimens.

A structural origin to the anomalous behavior appears likely. Transmission electron microscopy (TEM) studies of sputtered 500 Å films grown on ⟨100⟩ and ⟨110⟩ MgO (after chemical removal of the MgO) show the films are monocrystalline. Figure 1 shows a dark field image using the 220 reflection for the [001] oriented specimen. Contrast from structural displacement boundaries is clearly evident. Results from dark field contrast analysis are consistent with a $(\frac{1}{4})a_0\langle 110\rangle$ displacement vector across these boundaries [6,8]. Across these APBs, the oxygen lattice remains undisturbed, while the cation lattice is displaced, such that the system remains monocrystalline. The domains are very irregular in shape and size, ranging from 50 to 1000 Å, with an average dimension near 275 Å. Streaking in some diffraction patterns demonstrates that these boundaries are predominantly composed of segments on planes of the form {110}, but also on {100} planes [8]. Similar results are obtained for the ⟨110⟩ specimen. APBs have been observed in other spinel films grown on MgO by solid-state reaction [5], chemical vapor deposition [6], pulsed-laser deposition [7], and molecular-beam epitaxy [9].

It has frequently been demonstrated that thin films are formed by heterogeneous nucleation and growth [11]. Since in the present case the spinel unit cell is twice the size of the MgO unit cell, while the O lattice is the same size in both unit cells, the first sublayer of $Fe_3O_4$ platelets or islands which nucleate epitaxially on MgO can coalesce with improper stacking in the cation lattice. Once the regions meet only substantial diffusion would correct the ordering. It has been shown that APBs are formed where spinel nuclei coalesce in $Mg_2TiO_4$ films grown by solid-state reaction [5]. Therefore, these boundaries result from the intrinsic growth mechanism, suggesting that their presence is independent of preparation technique.

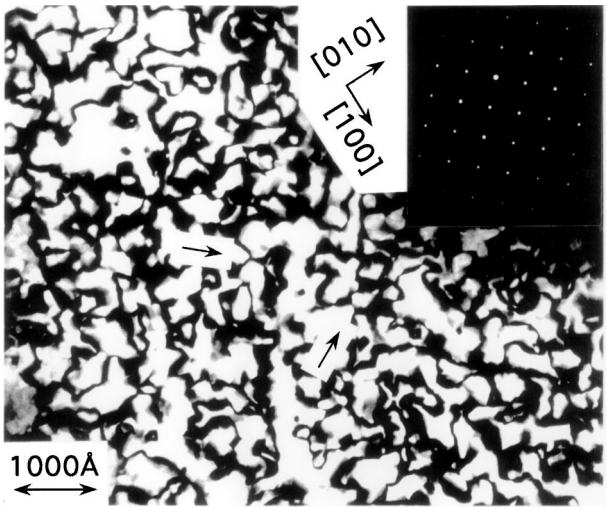


FIG. 1. Dark field TEM image using the 220 reflection for the [001] oriented 500 Å specimen. A selected area diffraction pattern is shown denoting crystallographic directions. Arrows point to some examples of locations where three APBs meet at a point as discussed in the text.

We now show that the anomalous magnetic behavior originates from the exchange interactions across the APBs. In the spinel oxides the predominant exchange interaction is superexchange between cations through the intervening oxygen [12]. Two main factors governing the strength of this antiferromagnetic interaction are (a) the angle ($\theta$) subtended by cation-anion-cation, in which a collinear arrangement (i.e., $\theta = 180°$) results in the strongest interaction and (b) the cation-anion distances. For orthoferrites, the exchange integral appears to be proportional to $\cos^2\theta$ [13]. In bulk $Fe_3O_4$ the exchange integral values are $J_{AB} = -22$ K, $J_{BB} = 3$ K, and $J_{AA} = -11$ K [10]. The interaction $J_{AB}$ is largest because the angle *A*-O-*B* is closest to 180°, but it also dominates because there are relatively more *AB* interactions (see Table I); $J_{BB}$ is positive due to additional Zener double exchange [10]. With a displacement of the form $(\frac{1}{4})a_0\langle 110\rangle$, and boundary planes of the form {110} and {100}, seven different arrangements of the cations exist across these boundaries. The four {110} types are described in Table I and one is illustrated in Fig. 2. The most significant aspects of the exchange interactions across these boundaries are (1) the angle *A*-O-*A* is substantially increased toward 180°, and the number of *AA* interactions is increased by about a factor of 2, relative to the normal lattice; (2) a significant number of *BB* interactions are created with an angle *B*-O-*B* of 180° [14]; (3) the angle *A*-O-*B* is unchanged, but the number of *AB* interactions is *reduced* by about a factor of 2 relative to the normal lattice. The three {100} types are very similar. It can be concluded that across the boundary the antiferromagnetic interaction between *A* sublattice atoms is greatly increased, a very strong antiferromagnetic interaction between cations on the *B* sublattice is created, and the normally dominant *AB* interaction is greatly reduced. Therefore, across the boundary the intrasublattice exchange interactions dominate, which would reverse the spin couplings, and the structural boundary would thus separate oppositely magnetized regions.

Experimental support for this model is supplied by magnetic imaging. The unique magnetic structure in these films is shown (Fig. 3) by Lorentz images using the Fresnel imaging mode on a 500 Å ⟨100⟩ oriented film. The contrast arises where the magnetization changes direction, the strength depending on the magnitude of the change and the distance over which it takes place. Bend contours are also visible. Remarkably, in applied fields of up to 6 kOe, which is well above the anisotropy field, no appreciable change was apparent in this quasirandom domain structure, which differentiates it from the familiar magnetization ripple [15]. Fringe-to-fringe spacings show a magnetic structure size about 2–4 times the structural

TABLE I. Summary of exchange interactions across all four different types of antiphase boundaries with a displacement of the form $(\frac{1}{4})a_0\langle 110\rangle$ and boundary planes of the form $\{110\}$ in $Fe_3O_4$. The columns describe the lattice sites of the two cations involved in the exchange interaction (int.), the number (#) of these interactions between different cations per unit cell area ($\sqrt{2}\,a_0^2$), the distances ($d$) between the two cations and the intermediate anion and between the two cations, and the relevant angle formed by the cation-anion-cation. All interactions with distances less than or equal to those in the bulk form are shown. Interactions which potentially could involve direct cation exchange are marked with (a) and interactions which are the same across the APB as found in bulk are marked by (b). A value of 0.375 is used for the $u$ parameter. The angles and distances do change with $u$, but using $u$ parameters typically found in spinels [12], variations would not be large enough to change our conclusions.

| Type | Int. $Fe_1Fe_2$ | # | $d$($Fe_1$-O) (Å) | $d$($Fe_2$-O) (Å) | angle (deg) | $Fe_1$-$Fe_2$ $d$ (Å) |
|---|---|---|---|---|---|---|
| I | *AA* | 12 | 1.82 | 3.48 | 151 | 5.14 |
| | *AA* | 10 | 1.82 | 3.48 | 121 | 4.69 |
| | *AA* | 4 | 1.82 | 1.82 | 109 | 2.97 |
| | *AA*[a] | 2 | 1.82 | 1.82 | 71 | 2.10 |
| | *BB* | 8 | 2.10 | 2.10 | 180 | 4.20 |
| | *BB*[b] | 12 | 2.10 | 2.10 | 90 | 2.97 |
| | *AB*[b] | 20 | 1.82 | 2.10 | 125 | 3.48 |
| | *AB*[a] | 4 | 1.82 | 2.10 | 55 | 1.82 |
| II | *AA* | 4 | 1.82 | 3.48 | 151 | 5.14 |
| | *AA* | 2 | 1.82 | 3.48 | 121 | 4.69 |
| | *BB* | 8 | 2.10 | 2.10 | 180 | 4.20 |
| | *BB*[b] | 12 | 2.10 | 2.10 | 90 | 2.97 |
| | *AB*[b] | 8 | 1.82 | 2.10 | 125 | 3.48 |
| III | *AA* | 8 | 1.82 | 3.48 | 151 | 5.14 |
| | *AA* | 8 | 1.82 | 3.48 | 121 | 4.69 |
| | *BB* | 8 | 2.10 | 2.10 | 180 | 4.20 |
| | *BB*[b] | 8 | 2.10 | 2.10 | 90 | 2.97 |
| | *AB*[b] | 16 | 1.82 | 2.10 | 125 | 3.48 |
| | *AB*[a] | 4 | 1.82 | 2.10 | 55 | 1.82 |
| IV | *AA* | 8 | 1.82 | 3.48 | 121 | 4.69 |
| | *AA* | 4 | 1.82 | 1.82 | 109 | 2.97 |
| | *BB* | 8 | 2.10 | 2.10 | 180 | 4.20 |
| | *BB*[b] | 16 | 2.10 | 2.10 | 90 | 2.97 |
| | *AB*[b] | 12 | 1.82 | 2.10 | 125 | 3.48 |
| Bulk | *AA* | 4 | 1.82 | 3.48 | 80 | 3.64 |
| | *BB* | 12 | 2.10 | 2.10 | 90 | 2.97 |
| | *AB* | 28 | 1.82 | 2.10 | 125 | 3.48 |

domain size. Similar results were observed for the $\langle 110\rangle$ oriented film. An important structural feature illustrated in Fig. 1 is the common occurrence of three boundaries intersecting at a point. In this case, the moment of one domain is antiferromagnetically coupled to the moments in the adjacent two domains, which in turn are antiferromagnetically coupled to each other. This indeterminate spin configuration leads to disorder in the spin arrangement, possibly producing the quasirandom magnetic structure observed.

In order to saturate the magnetization in $Fe_3O_4$, the magnetic field must be large enough to align all *B* site spins parallel to the field direction, while *A* site spins are antiparallel due to *AB* exchange coupling. In bulk crystals, this occurs at a relatively low field which only needs to be large enough to overcome the anisotropy and dipolar fields. However, in order to create this collinear arrangement of the spins in films the field must be large enough to overcome the strong exchange coupling across the APB which favors antiparallel *B* spins and antiparallel *A* spins on either side of the boundary. Exchange fields are very large and therefore the films remain unsaturated in fields as large as 70 kOe. As a demonstration of the field magnitude needed to saturate such a model of spins near an APB, we investigated a ferrimagnetic linear chain of spins [16] where the sign of the exchange has been reversed at the center. Zijlstra has presented a similar

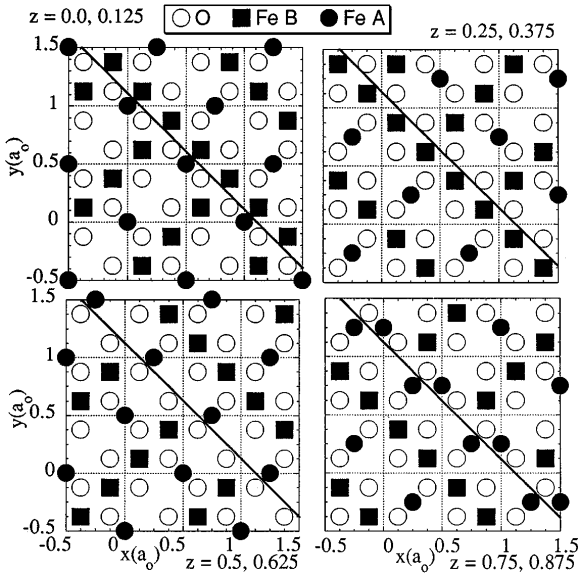


FIG. 2. Atomic locations at a type I APB described in Table I. The Fe *A* atoms are located at $z = 0$, $\frac{1}{4}$, $\frac{1}{2}$, and $\frac{3}{4}$, while Fe *B* and O atoms are located at $z = \frac{1}{8}$, $\frac{3}{8}$, $\frac{5}{8}$, and $\frac{7}{8}$.

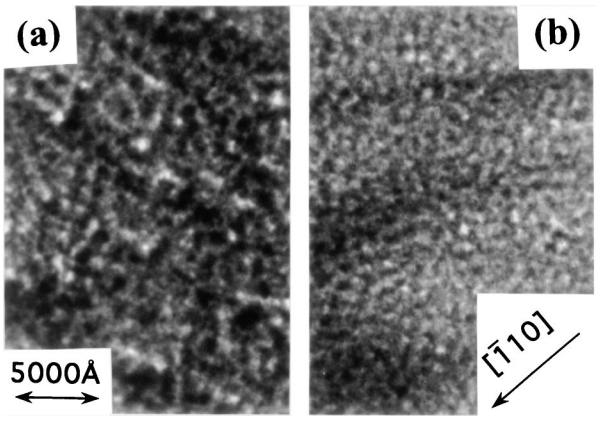


FIG. 3. Representative Lorentz microscopy images taken in the Fresnel mode of the [001] oriented specimen with the film plane rotated about the $[\bar{1}10]$ direction. Fields of 215 Oe (a) and 1160 Oe (b) are applied in the [110] direction.

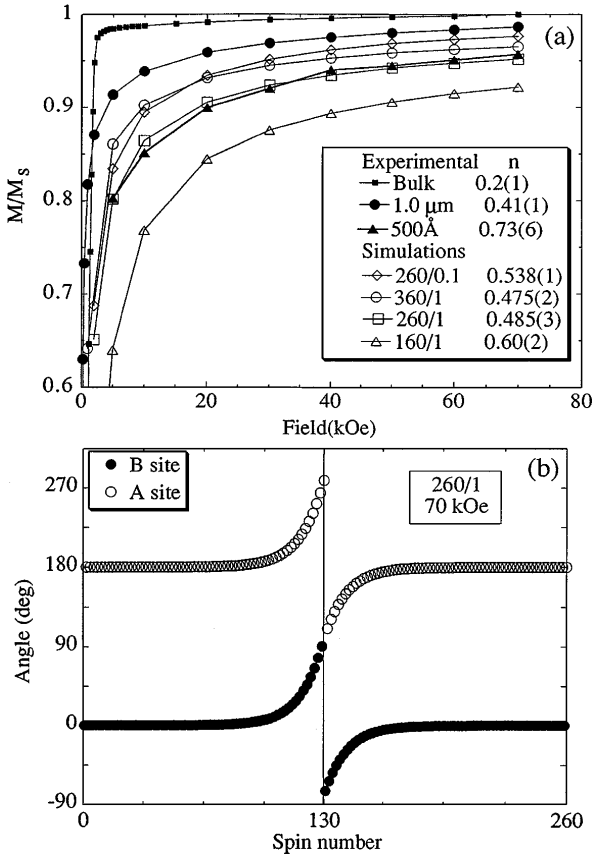


FIG. 4. (a) Magnetization, normalized to the bulk value, as a function of field, measured in the film plane along a ⟨100⟩ direction for 1 $\mu$m and 500 Å films grown on ⟨100⟩ MgO, and along an unknown crystallographic direction for a bulk crystal [1]. Similarly shown are calculations of the normalized magnetization of a ferrimagnetic linear chain of spins where the sign of the exchange has been reversed at the center. Also given are the number of spins in the chain and the magnitude of the exchange at the center normalized to the bulk magnitude (e.g., 260/1). The chain 260/10 is very similar to 260/1. The lines are visual guides. The magnetization fit parameter $n$ (see text) is listed. (b) The angle of the individual spins as a function of location in the chain with the field at 70 kOe.

model to describe the pinning of domain walls at APBs in ferromagnetic MnAl [17]. In the present case the free energy includes the exchange and Zeeman energies, and the moments have been adjusted to fit $Fe_3O_4$ parameters. The comparison of such a model to the magnetization of two films can be seen in Fig. 4, where very similar large saturation fields are required for both the films and the model. The effects of the domain size and the magnitude of the exchange at the boundary are shown. Remarkable agreement is seen between the 260 spin model simulation, where the separation between spins is about 1 Å in $Fe_3O_4$, and the 500 Å film, with a mean APB size of 275 Å. It is plausible that the difference between the 500 Å and 1 $\mu$m film in Fig. 4 is due to a greater structural domain size in the thicker film. A similar spin arrangement with similar high field differential susceptibility is observed in multilayers which simulate ferrimagnets [18]. An important similarity between the film, the ferrimagnetic chain, and the artificial ferrimagnet, is that using the equation $M = M_s(1 - b/H^n)$ to describe the approach to saturation of the magnetization ($M$) as a function of field ($H$), a value of the exponent ($n$) near 0.5 (see Fig. 4) is obtained as expected for competition between exchange and Zeeman energies [18]. A value of $n$ near 0.4 was obtained for unsaturated $NiFe_2O_4$ films [4]. The fits to the current experimental data (not shown) also included a small paraprocess correction, which was consistent with that experimentally observed in the bulk, and used H values from 10–70 kOe.

In summary, we have shown that the exchange coupling across antiphase boundaries in single crystal $Fe_3O_4$ films grown on MgO leads to unsaturated magnetization in magnetic fields over 2 orders of magnitude larger than the anisotropy field of bulk $Fe_3O_4$, and to quasirandom magnetic domain arrangements. Since the presence of the APBs results directly from the growth process of thin films, the anomalous magnetic properties should be intrinsic to these frequently studied films, independent of preparation technique.

This work was supported by NSF Grant No. DMR-9400439.

*Present address: IBM, 650 Harry Road, San Jose, CA 95120.

[1] D. T. Margulies *et al.*, Phys. Rev. B **53**, 9175 (1996).
[2] P. A. A. van der Heijden *et al.*, Mater. Res. Soc. Symp. Proc. **384**, 27 (1995).
[3] D. M. Lind *et al.*, Phys. Rev. B **45**, 1838 (1992).
[4] S. Venzke *et al.*, J. Mater. Res. **11**, 1187 (1996).
[5] D. Hesse, J. Vac. Sci. Technol. A **5**, 1696 (1987).
[6] A. G. Fitzgerald *et al.*, Thin Solid Films **35**, 201 (1976).
[7] S. Ramamurthy, P. G. Kotula, and C. B. Carter, Mater. Res. Soc. Symp. Proc. **343**, 517 (1994).
[8] M. L. Rudee, D. T. Margulies, and A. E. Berkowitz, Microsc. Microanal. **3**, 126 (1997).
[9] J. M. Gaines *et al.*, J. Magn. Magn. Mater. **165**, 439 (1997).
[10] E. De Grave *et al.*, Phys. Rev. B **47**, 5881 (1993).
[11] B. G. Orr *et al.*, Solid State Electron. **37**, 1057 (1994).
[12] E. W. Gortner, Philips Res. Rep. **9**, 295 (1954).
[13] G. A. Sawatzky *et al.*, J. Magn. Magn. Mater. **3**, 37 (1976).
[14] J. P. Jakubovics *et al.*, J. Appl. Phys. **49**, 2002 (1978).
[15] H. Hoffmann, IEEE Trans. Magn. **4**, 32 (1968).
[16] F. T. Parker and A. E. Berkowitz, Phys. Rev. B **44**, 7437 (1991).
[17] H. Zijlstra, IEEE Trans. Magn. **15**, 1246 (1979).
[18] B. Dieny *et al.*, J. Magn. Magn. Mater. **93**, 503 (1991).